

Publication II

This article was published in

R. K. Kaila and A. O. I. Krause, Autothermal reforming of simulated gasoline and diesel fuels, *Int. J. Hydrogen Energy* **31** (2006) 1934-1941.

© 2006 Elsevier

Reprinted with permission from Elsevier.

Autothermal reforming of simulated gasoline and diesel fuels

R.K. Kaila*, A.O.I. Krause

Laboratory of Industrial Chemistry, Helsinki University of Technology, P.O. Box 6100, FIN-02015 TKK, Finland

Received 30 August 2005; received in revised form 8 February 2006; accepted 29 April 2006

Available online 22 June 2006

Abstract

Autothermal reforming (ATR) of simulated fuels was studied with *n*-heptane, *n*-dodecane, toluene, and methylcyclohexane as model compounds for different fractions of gasoline and diesel on zirconia-supported Rh and Pt. A performance comparison was made on commercial nickel catalyst. No inhibiting effect was observed between the hydrocarbons on any catalyst, even though aliphatic hydrocarbons are more reactive than aromatics. The product selectivities obtained in ATR of simulated fuels could be calculated from the selectivities obtained in ATR of single hydrocarbons.

ATR of fuels has to be operated at high temperatures, which promotes thermal cracking. To prevent these side reactions active and selective catalysts are needed. The Rh/ZrO₂ catalyst showed high ATR activity and selectivity. Moreover, less coke was accumulated on the zirconia-supported noble metal catalysts than on the commercial nickel catalyst. Some deactivation of the rhodium and nickel catalysts was, however, observed.

© 2006 International Association for Hydrogen Energy. Published by Elsevier Ltd. All rights reserved.

Keywords: ATR; Thermoneutrality; Higher hydrocarbons; Simulated gasoline and diesel; Pt and Rh catalysts; Zirconia support

1. Introduction

Demand for hydrogen will increase dramatically in the future when new applications for fuel cells are commercialized. Hydrogen and synthesis gas (H₂ + CO) are already widely produced by steam reforming (STR) of methane in stationary systems. Although, methane can easily be utilized in the vicinity of natural gas pipelines, it must be compressed when it is transported and stored in vehicles. An easily delivered and safely storable hydrogen source, such as gasoline or diesel, would thus be preferable in mobile applications. The infrastructure for these fuels already exists, moreover. Hydrogen generation could be carried out anywhere using an on-board

reformer, and internal combustion engines could be replaced with more efficient fuel cell engines [1,2].

STR of higher hydrocarbons has been practiced for the last 40 years in locations where natural gas is not available [3]. Unfortunately, coke is formed in large amount on the conventional nickel catalysts [4]. In addition, nickel catalysts do not tolerate sulfur compounds [5,6]. Thus, more stable catalysts are required for commercial fuels to be used as a hydrogen source. Stable reforming catalysts would also find application in autothermal reforming (ATR), where the highly endothermic STR is combined with the exothermic partial oxidation (POX) reaction [7,8]. ATR is the preferred choice for vehicle applications of higher hydrocarbons owing to its short start-up time [6,8,9]. Moreover, the ATR product gas, containing mainly H₂, CO, CO₂, CH₄, and H₂O, can be utilized, for example, in solid oxide fuel cells (SOFC), albeit the selectivity to hydrogen

* Corresponding author. Tel.: +358 9 451 2666;
fax: +358 9 451 2622.

E-mail address: reetta.kaila@tkk.fi (R.K. Kaila).

is lower in ATR than in STR [10]. In addition, operation of ATR of *n*-heptane, at least, is thermally more stable than STR [11]. Still, ATR of hydrocarbon mixtures and liquid fuels has not been studied sufficiently.

In this work, ATR of higher hydrocarbons and their mixtures was studied in order to gain more insight into the suitability of liquid fuels as feed for ATR. Moreover, the interaction of hydrocarbons in simulated fuels was evaluated. *n*-Heptane and *n*-dodecane were used as model compounds for the *n*-alkane fractions of gasoline and diesel, and toluene and methylcyclohexane (MCH) as model compounds for the aromatic and cycloalkane fractions, respectively.

Zirconia-supported rhodium and platinum catalysts, and for comparison a commercial NiO/Al₂O₃ catalyst, were studied. Zirconia is noted for its stability [12]. In addition, as an acid–base bifunctional oxide it is less acidic than alumina [13]. Despite of these good features, zirconia has enjoyed only limited use as a support due to its low surface area. In recent years, especially mixed zirconia oxides have attracted much attention in various reactions [14,15]. The noble metals were chosen for their tolerance against coke formation and sulfur compounds [4,16–18].

2. Experimental

2.1. Thermodynamics

Thermodynamics of the ATR reactions of *n*-heptane, *n*-dodecane, toluene, and MCH were calculated with HSC Chemistry version 5.11 [19] to determine the reaction conditions under which a thermoneutral total reaction in ATR could be achieved.

2.2. Catalysts

Two noble metal catalysts, 0.5 wt% Rh/ZrO₂ and 0.5 wt% Pt/ZrO₂, were prepared by dry impregnation using a 10 wt% Rh(NO₃)₃ solution in diluted (5 wt%) nitric acid (Sigma-Aldrich) and a Pt(NH₄)₄(NO₃)₂ solution (99%, Strem Chemicals). The ZrO₂ support (MEL Chemicals EC0100) was ground to particle size 0.25–0.3 mm and calcined at 900 °C for 16 h. After impregnation, the catalysts were dried at room temperature for 4 h and at 100 °C overnight, followed by calcination at 700 °C for 1 h (heating rate 80 °C/h). The noble metal content of the catalysts was characterized with inductively coupled plasma-atomic emission spectroscopy (ICP-AES). A commercial 15 wt% NiO/Al₂O₃ catalyst (0.2–0.3 mm) was used for comparison.

2.3. Catalyst testing in ATR reactions

Testing of the catalysts in ATR reactions was performed in a tubular quartz reactor with temperature set to 700–900 °C and with 0.1–0.3 g of catalyst. The reactor temperature was increased stepwise, and finally it was set back to the initial temperature (700 °C) to investigate the catalyst deactivation. After the ATR cycle, the catalyst was regenerated with air and the product was analyzed. The formation of carbon dioxide and water during the regeneration step indicated coke accumulation. The regeneration step was followed by a second ATR cycle.

The feed consisted of *n*-heptane (H) ($\geq 99.5\%$, Fluka), *n*-dodecane (D) (99 + %, Sigma-Aldrich), toluene (T) ($\geq 99.7\%$, Riedel-de Haën), MCH (M) ($\geq 99\%$, Merck), or simulated fuels, plus water and air. Simulated fuels were prepared from the model compounds with the following molar ratios: (A) T/H = 40/60, (B) T/D = 30/70, (C) T/H/D = 20/30/50, and (D) T/H/M = 20/30/50. The aromatic content varied between 14 and 38 wt%. The ATR experiments were started with single model compounds in order to understand their characteristics.

The H₂O/C and O₂/C feed ratios of the ATR experiments were 3 mol/mol and 0.34 mol/mol, respectively. These ratios were selected, on the basis of reaction condition optimization and thermodynamic calculations, to provide a thermoneutral ATR of *n*-heptane and *n*-dodecane at 700 °C and to minimize coke deposition. The hydrocarbons and water were vaporized and mixed with air prior to their introduction to the reactor. The total flow rate of the reactants was 300 cm³/min (NTP), and the feed was diluted with argon to a total flow rate of 900 cm³/min (NTP). For comparative purpose, thermal experiments without any catalyst were performed with temperatures set to 600–900 °C.

2.4. Product analysis

The product flow was diluted with nitrogen (900 cm³/min NTP) to allow reliable detection of the hydrocarbons [20]. The diluted stream was analyzed with a Fourier transform infrared spectrometer (FT-IR) equipped with a Peltier-cooled MCT detector and multicomponent analysis software. The temperature of the sample cell was set to 230 °C to keep the higher hydrocarbons in the gas phase. All oxygen was assumed to be consumed, since the O₂/C feed ratio was less than the stoichiometric ratio of the POX reactions. The amount of hydrogen formed was calculated from the

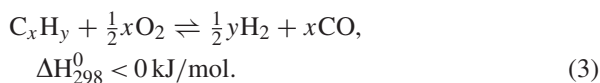
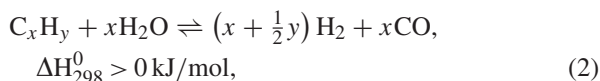
mass balances on the basis of the measured dry gas flow rate. The selectivity was calculated with Eq. (1), where n_i is the molar amount of product i .

$$S_i = \frac{n_i}{\sum n_i}. \quad (1)$$

3. Results and discussion

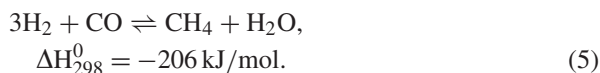
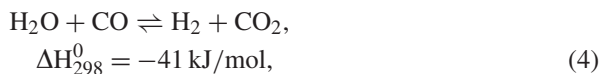
3.1. Thermodynamics of thermoneutral ATR

The ATR feed consisted of hydrocarbons, water, and air. Consequently, in addition to the endothermic STR (Eq. (2)), exothermic POX (Eq. (3)) takes place in the reformer



The absolute value of STR and POX reaction enthalpies increases noticeably with the chain length of the hydrocarbon (Table 1). Since STR is highly endothermic, the reactor has to be heated substantially, especially when water is fed in excess ($H_2O/C > 1$ mol/mol). However, when oxygen is added (ATR), the total system can be driven to thermoneutral conditions. The optimal O_2/C feed ratios and the STR and POX conversions in thermoneutral ATR at 700 °C are presented in Table 1.

The contribution of side reactions, such as water gas shift (WGS) reaction (Eq. (4)) and methanation (Eq. (5)), to the product distribution of the ATR reactions was studied as well. When these exothermic reactions are included in the calculations of thermoneutrality, the optimal O_2/C feed ratios at 700 °C decrease slightly (0.33 mol/mol for n -heptane ATR). At the same time, the hydrocarbon conversions via POX decrease slightly.



At temperatures above 815 °C, the WGS equilibrium (Eq. (4)) is shifted towards carbon monoxide and water. As a result of the WGS reaction, the equilibrium H_2/CO molar ratio of the ATR product increases up to about 5 mol/mol at 700 °C when water is fed in excess (3 mol/mol C). Owing to the water excess, the equilibrium conversion of carbon monoxide in WGS at 700 °C

is about 60% with all studied hydrocarbons. The methanation equilibrium does not affect the product distribution at temperatures above 616 °C.

3.2. Thermal experiments of single hydrocarbons

Thermal experiments were performed under optimized ATR conditions in the absence of catalyst. The conversions of n -heptane, n -dodecane, and MCH increased with temperature, approaching 100% at 800–850 °C, with n -dodecane the most reactive hydrocarbon. Toluene started to react only at 800 °C and was the only hydrocarbon that did not react completely (Fig. 1).

The main products in the thermal experiments were hydrogen, carbon oxides, ethene, methane, and propane. Except for propane, the amount of products increased with temperature and the hydrocarbon conversion. Hydrogen was formed in greatest amount in reactions of n -dodecane and least amount in reactions of toluene. Most ethene was formed in reactions of n -heptane, and hardly any in reactions of toluene. The formation of ethene accelerated with temperature until 900 °C, when it finally declined.

Light hydrocarbons and hydrogen were formed via thermal cracking, whereas carbon oxides were formed mainly through oxidation reactions. However, in the absence of catalyst the conversion of oxygen reached 100% only at 900 °C.

3.3. ATR of single hydrocarbons

ATR of n -heptane, n -dodecane, toluene, and MCH was studied on the commercial nickel catalyst with GHSV 3.6×10^5 1/h. The conversion of n -dodecane was almost 100% over the whole temperature range investigated, whereas the conversions of n -heptane, MCH, and toluene improved with temperature (Fig. 2). Thus, n -dodecane was the most reactive hydrocarbon, and toluene the most stable, in agreement with the results of the thermal experiments and as expected from the thermodynamic calculations.

The main products of ATR of all hydrocarbons were hydrogen, carbon monoxide, and carbon dioxide (Table 2). The selectivity to hydrogen increased with temperature and conversions of n -heptane, n -dodecane, toluene, and MCH achieving the maximum selectivities of 57%, 62%, 45%, and 51% at about 850 °C, respectively. The H_2/CO molar ratio of the ATR product over the whole temperature range was lower than the thermodynamic ratio (5 mol/mol at 700 °C). Thus, the thermodynamic equilibrium of ATR was not achieved—not

Table 1

Thermodynamic data calculated for thermoneutral ATR of toluene, MCH, *n*-heptane, and *n*-dodecane at 700 °C

Hydrocarbon	ΔH_{700} (kJ/mol)		Optimal O ₂ /C feed ratio (mol/mol)	Conversion in thermoneutral ATR (mol%)		H ₂ /CO ratio in product (mol/mol)		
	STR	POX		STR	POX	STR	POX	ATR
Toluene	925	−808	0.27	46.6	53.4	1.57	0.57	1.05
MCH	1145	−592	0.33	34.2	65.8	2.00	1.00	1.48
<i>n</i> -Heptane	1180	−553	0.34	31.9	68.1	2.14	1.14	1.48
<i>n</i> -Dodecane	2122	−849	0.36	28.6	71.4	2.08	1.08	1.38

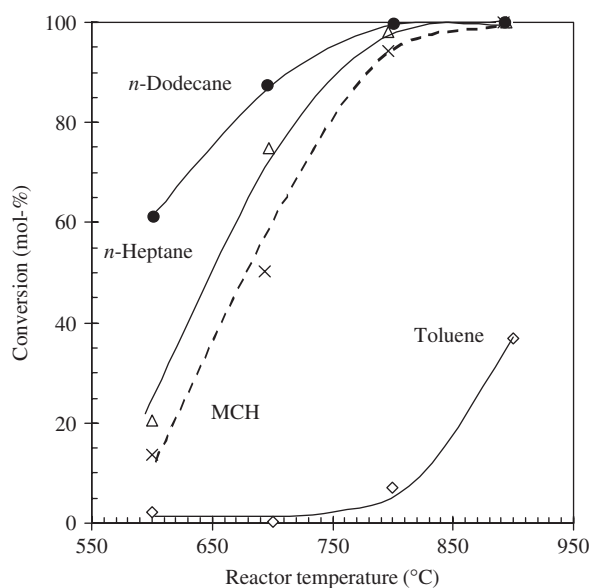


Fig. 1. Cracking conversions of *n*-dodecane (●), *n*-heptane (△), MCH (×), and toluene (◇) in ATR conditions (H₂O/C = 3 mol/mol, O₂/C = 0.34 mol/mol, V_{reactants} = 300 ml/min (NTP)).

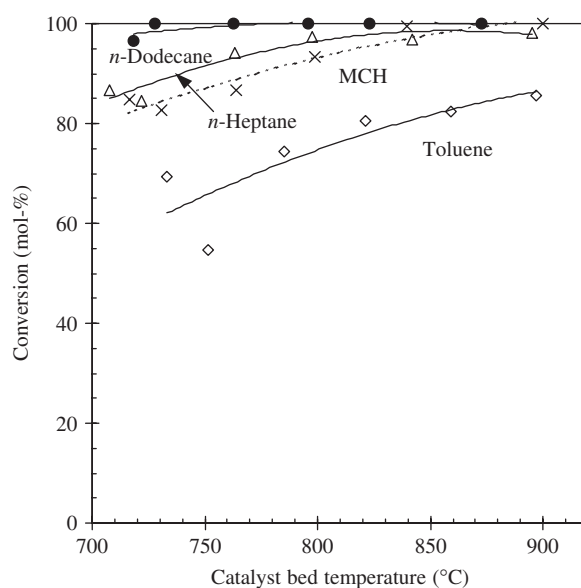


Fig. 2. ATR conversions of *n*-dodecane (●), *n*-heptane (△), MCH (×), and toluene (◇) on 15 wt% NiO/Al₂O₃ (H₂O/C = 3 mol/mol, O₂/C = 0.34 mol/mol, GHSV = 3.6 × 10⁵ 1/h).

even at higher temperatures, where complete hydrocarbon conversions were obtained. However, the amount of carbon dioxide decreased, while the amount of carbon monoxide increased with temperature due to the WGS equilibrium.

As side products, ethene, methane, and small amounts of other light hydrocarbons were formed in ATR of the aliphatic hydrocarbons. Furthermore, in reactions of *n*-heptane and MCH, the amounts of ethene and methane increased with temperature, indicating that thermal cracking became more significant in the course of the experiment; in ATR of *n*-dodecane, in turn, the amount of ethene decreased with the temperature. Thus, thermal cracking seems to take place always when the ATR conversion of the aliphatic hydrocarbons is incomplete, besides accelerating with temperature.

Virtually no side products were detected in ATR of toluene since toluene did not react via thermal cracking. However, in reactions of toluene high concentrations of carbon dioxide were formed due to the use of a higher O₂/C molar ratio (0.34 mol/mol) than was required for thermoneutrality (Table 1). Moreover, the total reaction of toluene was more exothermic than that of the other hydrocarbons over the whole temperature range, in agreement with the thermodynamics. Flytzani-Stephanopoulos and Voecks [7] noticed similar temperature differences between aliphatic and aromatic hydrocarbons, which they attributed to the appearance of carbon in the catalyst bed.

Indeed, coke was accumulated on the nickel catalyst, which caused a pressure drop over the reactor, especially in ATR of *n*-heptane and MCH where

Table 2

Conversions and selectivities in ATR of single hydrocarbons on 15 wt% NiO/Al₂O₃ (0.2 g) with temperature set at 700 °C

Hydrocarbon	<i>T</i> (°C)	Conversion (mol%)	Selectivity (mol%)						
			H ₂	CO	CO ₂	Ethene	Methane	Alkenes	Alkanes
Toluene	721	71.0	36.3	25.7	36.3	0.0	0.2	0.1	0.0
MCH	731	82.6	48.8	27.5	22.2	0.2	0.1	0.1	0.3
<i>n</i> -Heptane	722	85.0	53.3	20.0	19.0	2.6	2.0	2.6	0.4
<i>n</i> -Dodecane	719	99.9	59.9	18.4	20.4	0.0	0.1	0.0	0.0

Table 3

Product selectivities in ATR of simulated fuels on 15 wt% NiO/Al₂O₃ (0.1 g) at 800 °C

Feed mixture	Hydrocarbon composition (mol%)			Product selectivity (mol%)			
	Toluene	<i>n</i> -Heptane	<i>n</i> -Dodecane	H ₂	CO	CO ₂	Ethene
A	40	60	0	44.7	28.7	19.3	4.2
B	30	0	70	61.7	14.8	20.5	1.4
C	20	30	50	62.9	11.9	20.9	2.1

thermal cracking intermediates were present. Moreover, the coke led to catalyst deactivation and thereby further promoted thermal cracking reactions. The ATR cycle was followed by a regeneration step and a second ATR cycle. In the second ATR cycle, the carbon dioxide content of the product was decreased. Evidently, then, the coke was also oxidized from the catalyst surface during the first ATR cycle increasing the selectivity to carbon dioxide, and to carbon monoxide through WGS equilibrium. These findings confirm the assumption of carbon formation and oxidation on the catalyst surface [7], yielding an exothermic total reaction, especially, in the ATR of toluene.

3.4. ATR of simulated fuels

ATR of simulated fuels was studied on Rh/ZrO₂ and Pt/ZrO₂, and for comparison on the NiO/Al₂O₃ catalyst.

The effect of aromatic hydrocarbons on ATR selectivities was studied on the nickel catalyst with a series of simulated fuels (A, B, and C) containing 20–40 mol% (14–38 wt%) toluene. The selectivities to carbon oxides increased and the selectivity to hydrogen decreased with the content of toluene (Table 3). Ethene was mainly formed in ATR of the toluene–*n*-heptane mixture (A) and least in ATR of the toluene–*n*-dodecane mixture (B). Thus, the selectivity to thermal cracking products increased with the content of *n*-heptane, and was not affected by the content of toluene, as was characteristic

for these hydrocarbons. Highest selectivities to the products of interest were achieved with the mixture of toluene and *n*-dodecane (B), which simulated diesel.

In ATR of simulated gasoline (mixture D) and diesel (mixture B), high-hydrogen selectivities and almost complete hydrocarbon conversion were achieved on Rh/ZrO₂ and NiO/Al₂O₃ catalysts over the whole temperature range studied, and virtually no side products were formed (Table 4, for simulated gasoline). On Pt/ZrO₂ catalyst, on the other hand, the hydrocarbon conversions and product selectivities to hydrogen and carbon monoxide were lower, and thermal cracking took place. Similar product selectivities to those on rhodium and nickel catalysts were, however, achieved on the platinum catalyst when the temperature was raised up to 850–900 °C (Table 5). The conversion of water and the selectivity to carbon dioxide decreased with increase in temperature, which likely was due to the WGS equilibrium that was shifted towards carbon monoxide and water. This affected also the H₂/CO molar ratio of the product, which decreased when the temperature was raised.

In a comparison of the catalyst bed temperatures at the set temperature of 700 °C (Table 4), the total ATR reaction with simulated fuels was observed to be highly exothermic on the platinum catalyst, but endothermic on the rhodium catalyst. Moreover, the large amounts of carbon oxides and water formed on the platinum catalyst indicated that exothermic oxidation reactions were

Table 4

Conversions and selectivities in ATR of simulated gasoline on 15 wt% NiO/Al₂O₃, 0.5 wt% Pt/ZrO₂, and 0.5 wt% Rh/ZrO₂ catalysts (0.2 g) with temperature set at 700 °C

Catalyst	Catalyst bed temperature (°C)	Conversion (mol%)				Selectivity (mol%)				
		<i>n</i> -Heptane	MCH	Toluene	Water	H ₂	CO	CO ₂	Ethene	Methane
Ni/Al ₂ O ₃	712	98.8	99.1	98.8	14.8	56.3	23.7	19.3	0.0	0.6
Pt/ZrO ₂	766	52.3	59.6	28.7	−0.4	7.2	50.7	31.1	3.9	2.3
Rh/ZrO ₂	685	95.0	95.5	95.9	19.4	55.1	25.4	18.3	0.0	1.0

Table 5

Conversions and selectivities in ATR of simulated gasoline on 15 wt% NiO/Al₂O₃, 0.5 wt% Pt/ZrO₂, and 0.5 wt% Rh/ZrO₂ catalysts (0.2 g) with temperature set at 900 °C

Catalyst	Catalyst bed temperature (°C)	Conversion (mol%)				Selectivity (mol%)				
		<i>n</i> -Heptane	MCH	Toluene	Water	H ₂	CO	CO ₂	Ethene	Methane
Ni/Al ₂ O ₃	873	100.0	100.0	98.3	10.7	54.9	30.3	13.5	0.4	0.8
Pt/ZrO ₂	893	100.0	100.0	80.7	5.6	41.6	33.6	13.1	5.2	4.7
Rh/ZrO ₂	869	100.0	100.0	96.0	14.1	56.9	27.3	13.4	0.8	1.4

taking place, which decreased the STR/POX reaction ratio. The conversion of water on platinum catalyst became negative (Table 4) and ATR could not be operated thermoneutrally. On rhodium, on the other hand, the conversion of water was highest, which indicated that rhodium was most active for STR, as is reported e.g. by Wieland et al. [8] for rhodium and platinum catalyst activities in STR and POX reactions, respectively.

No competition or inhibition of the hydrocarbons took place on any catalyst. The conversions in ATR of single hydrocarbons (Fig. 3) were comparable with those of their mixture (Fig. 4). Moreover, the product selectivities in ATR of simulated gasoline (mixture D), as well as simulated diesel (mixture B), were alike the weighted averages calculated from selectivities achieved in the experiments with single hydrocarbons (Fig. 5, for simulated diesel). The deactivation of the catalyst, however, weakened the congruency, especially on the nickel catalyst at lower temperatures.

In ATR experiments of simulated fuels, very little coke was accumulated on both noble metal catalysts, unlike in the nickel experiments where the pressure drop over the reactor increased slightly with time. Slight deactivation was noticed during the ATR experiments on the nickel and rhodium catalysts, however, and the deactivation was stronger in ATR of the simulated gasoline than in ATR of the simulated diesel. Moreover, the nickel catalyst particles exhibited some crumbling during the experiment, perhaps due to

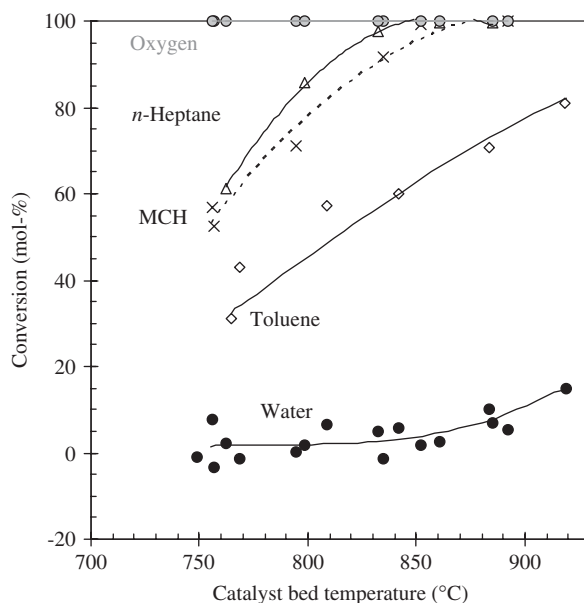


Fig. 3. Conversions of MCH (×), *n*-heptane (△), toluene (◇), water (●), and oxygen (○) in ATR of single hydrocarbons on 0.5 wt% Pt/ZrO₂ (H₂O/C = 3 mol/mol, O₂/C = 0.34 mol/mol, GHSV = 3.6 × 10⁵ l/h).

formation of whisker carbon under the active nickel atoms [4]. Zirconia-supported noble metal catalysts were thus considerably more stable towards coke formation than was the nickel catalyst. However, in

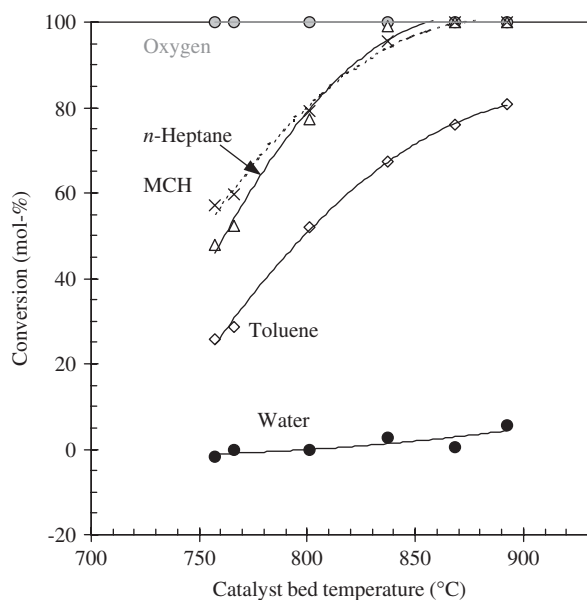


Fig. 4. Conversions of MCH (\times), *n*-heptane (Δ), toluene (\diamond), water (\bullet), and oxygen (\odot) in ATR of simulated gasoline on 0.5 wt% Pt/ZrO₂ (H₂O/C=3 mol/mol, O₂/C=0.34 mol/mol, GHSV = 3.6×10^5 1/h).

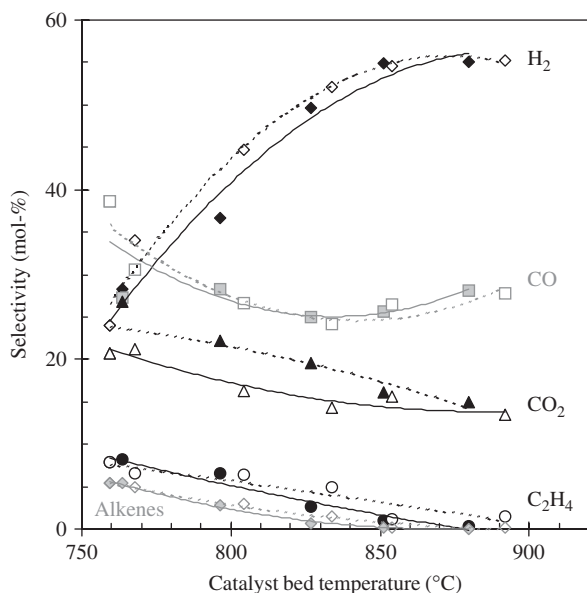


Fig. 5. Measured (filled symbol) and calculated (empty symbol) product selectivities (H₂ (\diamond), CO (\square), CO₂ (Δ), C₂H₄ (\circ), and selectivities to other alkenes (\diamond)) in ATR of simulated diesel on 0.5 wt% Pt/ZrO₂ (H₂O/C=3 mol/mol, O₂/C=0.34 mol/mol, GHSV = 3.6×10^5 1/h).

ATR of simulated gasoline on the rhodium catalyst, a significant decrease in hydrocarbon conversions and hydrogen selectivity was noticed during the second

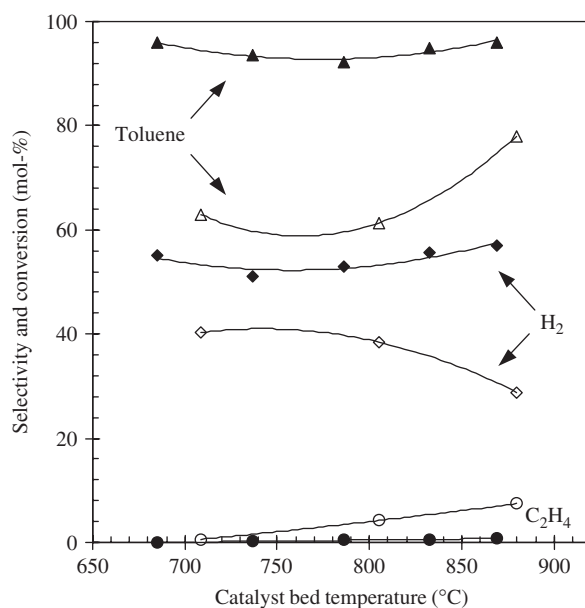


Fig. 6. Toluene conversions (Δ) and product selectivities (H₂ (\diamond) and C₂H₄ (\circ)) in ATR of simulated gasoline on the 0.5 wt% Rh/ZrO₂ catalyst during first (filled symbol) and second (empty symbol) ATR cycle (H₂O/C = 3 mol/mol, O₂/C = 0.34 mol/mol, GHSV = 3.6×10^5 1/h).

ATR cycle (Fig. 6). In fact, some decrease in toluene conversion was noticed at lower temperatures (750 °C) already during the first ATR cycle (Fig. 6). However, the hydrocarbon conversions and selectivities to main products were in the second ATR cycle still higher than in ATR reactions on the pure ZrO₂ support. Thus, some activity was left also during the second ATR cycle, even though the measured Rh content of the catalyst was decreased substantially. Likely, volatile rhodium compounds were formed in the oxidative reforming conditions, and these evaporated from the catalyst surface at high temperatures (850–900 °C) [21]. Consequently, the thermal stability of Rh/ZrO₂ catalyst needs to be improved before its high activity and selectivity can be exploited in high temperature commercial applications.

4. Conclusions

ATR of higher hydrocarbons can be operated thermoneutral, which is an important issue when large-scale applications are designed. Moreover, coke accumulation on the catalyst is decreased compared to STR.

Since aromatics are more stable hydrocarbons than aliphatics, the ATR reaction temperature has to be raised when simulated fuels are used as feedstock. However,

thermal cracking accelerates with temperature and takes place especially when the conversion of aliphatic hydrocarbons is incomplete. Therefore, thermal cracking will be present also in ATR of commercial fuels if the catalyst activity is not high enough and the reactions cannot be operated at lower temperatures.

In the studies on simulated fuels, no competition between the studied hydrocarbons was noticed on any catalyst. Thus, the selectivities achieved in ATR of simulated fuels can be calculated from the results obtained in ATR reactions of single hydrocarbons. Catalyst deactivation reduces the congruency, however, especially at lower temperatures.

The 0.5 wt% Rh/ZrO₂ catalyst was as active as the commercial 15 wt% NiO/Al₂O₃ catalyst in ATR of simulated fuels. Rhodium was also most active for STR, whereas its oxidation activity was low compared with that of 0.5 wt% Pt/ZrO₂. Furthermore, less coke was accumulated on the zirconia-supported catalysts than on the conventional nickel catalyst. Even so, deactivation of the nickel as well as the rhodium catalysts was noticed during the experiments, whereas platinum maintained its stability.

Acknowledgments

Financial support was received from VTT (Technical Research Centre of Finland) and Tekes (Finnish Funding Agency for Technology and Innovation).

References

- [1] Brown LF. A comparative study of fuels for on-board hydrogen production for fuel cell-powered automobiles. *Int J Hydrogen Energy* 2001;26:381–97.
- [2] Pettersson LJ, Westerholm R. State of the art of multi-fuel reformers for fuel cell vehicles: problem identification and research needs. *Int J Hydrogen Energy* 2001;26:243–64.
- [3] Rostrup-Nielsen JR, Bak Hansen J-H, Aparigio LM. Reforming of hydrocarbons into synthesis gas on supported metal catalysts. *Sekiyu Gakkaishi* 1997;40(5):366–77.
- [4] Kochloefl K. Steam reforming. In: Ertl G, Knözinger H, Weitkamp J, editors. *Handbook of heterogeneous catalysis*, vol. 4. Weinheim: Wiley VCH; 1997. p. 1819–31.
- [5] Rostrup-Nielsen JR. Catalytic steam reforming. In: Anderson JR., Boudart M, editors. *Catalysis: science and technology*, vol. 4. Berlin, Heidelberg, New York, Tokyo: Springer; 1984. p. 1–117.
- [6] Rostrup-Nielsen JR. Conversion of hydrocarbons and alcohols for fuel cells. *Phys Chem Chem Phys* 2001;3:283–8.
- [7] Flytzani-Stephanopoulos M, Voecks GE. Autothermal reforming of aliphatic and aromatic hydrocarbon liquids. *Int J Hydrogen Energy* 1983;8(7):539–48.
- [8] Wieland S, Baumann F, Ahlborn R. Process for the autothermal catalytic steam reforming of hydrocarbons. US 2002/0009408 A1, 2002.
- [9] Aasberg-Petersen K, Bak Hansen J-H, Christensen TS, Dybkjaer I, Seier Christensen P, Stub Nielsen C, et al. Technologies for large-scale gas conversion. *Appl Catal A: General* 2001;221:379–87.
- [10] Ormerod RM. Fuels and fuel processing. In: Singhal SC, Kendall K, editors. *High temperature solid oxide fuel cells: fundamentals, design and applications*. Cornwall: Elsevier; 2003. p. 333–61.
- [11] Kaila RK, Krause AOI. Reforming of higher hydrocarbons. *Stud Surf Sci Catal* 2004;147:247–52.
- [12] Nagaoka K, Seshan K, Aika K, Lercher JA. Carbon deposition during carbon dioxide reforming of methane-comparison between Pt/Al₂O₃ and Pt/ZrO₂. *J Catal* 2001;197(1):34–42.
- [13] Yamaguchi T. Application of ZrO₂ as a catalyst and a catalyst support. *Catal Today* 1994;20:199–218.
- [14] Kusakabe K, Sotowa K-I, Eda T, Iwamoto Y. Methane steam reforming over Ce-ZrO₂-supported noble metal catalysts at lower temperature. *Fuel Process Technol* 2004;86:319–26.
- [15] Reddy BM, Khan A. Recent advances on TiO₂-ZrO₂ mixed oxides as catalysts and catalyst supports. *Catal Rev* 2005;47:257–96.
- [16] Palm C, Cremer R, Peters R, Stolten D. Small-scale testing of precious metal catalyst in the autothermal reforming of various hydrocarbon feeds. *J Power Sources* 2002;106:231–7.
- [17] Claridge JB, Green MLH, Tsang SC, York APE, Ashcroft AT, Battle PD. A study of carbon deposition on catalysts during the partial oxidation of methane to synthesis gas. *Catal Lett* 1993;22:299–305.
- [18] Krumpelt M, Krause TR, Carter JD, Kopasz JP, Ahmed S. Fuel processing for fuel cell systems in transportation and portable applications. *Catal Today* 2002;77:3–16.
- [19] Roine A. HSC chemistry for windows 5.11. Outokumpu Research Oy, 2003.
- [20] Tate JD, Jaakkola P. The use of a portable low-resolution FT-IR for industrial gas analysis. *J Process Anal Chem* 2000;5(1,2):15–28.
- [21] Zhu J. Catalytic partial oxidation of methane to synthesis gas over ZrO₂-based defective oxides. Enschede: Printpartners Ipskamp B.V.; 2005 119p.